Flow Resistance and Drag Forces Due to Multiple Adherent Leukocytes in Postcapillary Vessels

Gary B. Chapman* and Giles R. Cokelet#
*Department of Biochemistry and Biophysics and #Department of Pharmacology and Physiology, University of Rochester, Rochester, New York 14642 USA

ABSTRACT Computational fluid dynamics was used to model flow past multiple adherent leukocytes in postcapillary size vessels. A finite-element package was used to solve the Navier-Stokes equations for low Reynolds number flow of a Newtonian fluid past spheres adhering to the wall of a cylindrical vessel. We determined the effects of sphere number, relative geometry, and spacing on the flow resistance in the vessel and the fluid flow drag force acting to sweep the sphere off the vessel wall. The computations show that when adherent leukocytes are aligned on the same side of the vessel, the drag force on each of the interacting leukocytes is less than the drag force on an isolated adherent leukocyte and can decrease by up to 50%. The magnitude of the reduction depends on the ratio of leukocyte to blood vessel diameter and distance between adherent leukocytes. However, there is an increase in the drag force when leukocytes adhere to opposite sides of the vessel wall. The increase in resistance generated by adherent leukocytes in vessels of various sizes is calculated from the computational results. The resistance increases with decreasing vessel size and is most pronounced when leukocytes adhere to opposite sides of the vessel.

INTRODUCTION

Firm adhesion of leukocytes to the venular endothelium is required for leukocytes to migrate from the lumen of the blood vessel to the surrounding tissue, where the immune response occurs. Intravital microscopy has clearly demonstrated that leukocytes adhere to the wall of postcapillary venules whose diameters may approach the diameter of the leukocyte. We have demonstrated that the presence of an adherent leukocyte disturbs the fluid flow in the vessel (Chapman and Cokelet, 1997) and have examined the impact of fluid flow past a single adherent spherical leukocyte (Chapman and Cokelet, 1996). However, leukocytes may adhere within close proximity to each other in vivo (House and Lipowsky, 1987), so that the leukocytes no longer behave as independent particles. The goal of this study is to determine the hemodynamics of multiple interacting adherent leukocytes.

This study examines two hemodynamic parameters. The first parameter is the drag force on the leukocyte exerted by blood flow past the adherent leukocyte. The drag force is important because a counterforce must be generated by receptor-ligand bonds between the surface of the leukocyte and the endothelium if the leukocyte is to adhere (Springer, 1994). If there is an insufficient number of bonds, the leukocyte will not adhere firmly to the vessel wall (Bell, 1978).

Received for publication 27 October 1997 and in final form 17 February 1998.

Address reprint requests to Dr. Giles Cokelet, Department of Pharmacology and Physiology, University of Rochester, 601 Elmwood Avenue, Rochester, NY 14642. Tel.: 716-275-5283; Fax: 716-244-9283; E-mail: cokelet@pharmacol.rochester.edu.

0006-3495/98/06/3292/10 $2.00

The second parameter this study addresses is the pressure drop across the adherent leukocytes. Because the leukocyte and blood vessel diameters are comparable, there can be an adverse effect on blood flow through the vessel containing adherent leukocytes. If blood flow is to be kept constant, the pressure drop forcing the fluid along the vessel must increase when leukocytes adhere to the vessel wall. The flow resistance (ratio of pressure drop to flow rate) in a vessel can affect blood flow distribution in a network of vessels. Whole organ studies have shown that leukocytes, when activated, increase their whole blood resistance contribution from 20% to 50–60% in skeletal muscle (Sutton and Schmid-Schönbein, 1992). There are several mechanisms that might account for this increase in resistance, such as capillary plugging (Warnke and Skalak, 1990), red blood cell train formation (Thompson et al., 1989), and leukocyte adhesion (House and Lipowsky, 1987; Chapman and Cokelet, 1997). The relative contribution of leukocyte-endothelial adhesion to this increase in resistance is unknown.

Few studies have addressed the impact of leukocyte adhesion on the flow resistance in vessels. Measurement of pressure drops in postcapillary vessels requires dual micropipette pressure measurements, a tedious and time-consuming procedure whose difficulty increases with decreasing vessel diameters. It is easier to measure the pressure drop in larger vessels (diameters greater than 20 μm), but adherent leukocytes have a smaller effect on the pressure drop as the diameter increases. Using micropipette pressure determinations, House and Lipowsky (1987) estimate that leukocyte adhesion increases single vessel resistance up to 80%. However, the range of vessel diameters studied was limited to between 25 and 49 μm. In addition, the effects of geometrical arrangement and number of adherent leukocytes on the change in resistance were not investigated.

Large-scale models have also been used to calculate the increase in resistance generated by multiple adherent leukocytes (Bagge et al., 1986). Bagge et al. measured the resistance increase, for a sphere-to-vessel diameter ratio of 0.4, for various geometrical arrangements. They showed that the resistance could increase more than fourfold when the spheres adhered in rings to maximize their impact on flow. Unfortunately, Bagge et al. did not address the impact of adherence in vessels of other sizes, and the geometrical arrangement and number of adherent spheres examined were limited.

A third method of investigating the change in resistance due to adherent leukocytes involves the use of computational fluid dynamics (CFD). We have used CFD to investigate the impact of a single adherent leukocyte and have shown that the largest increase in resistance occurs in the smallest size vessels (Chapman and Cokelet, 1997). We know of no three-dimensional solutions that address the impact of multiple leukocyte adhesion. In this study we use a CFD package (CFD Research Corp., Huntsville, AL) to examine how the drag force on, and pressure drop across, adherent leukocytes change with the number and relative position of leukocytes. The accuracy of the package has been verified for single adherent leukocytes in vessles of various sizes (Chapman and Cokelet, 1996, 1997). The computational package has an advantage in that precise locations and numbers of leukocytes are specified so that correlations that are difficult to obtain from in vivo experiments can be developed.

METHODS

A finite volume solution package (CFD-ACE; CFD Research Corp.) on a SunSparc 20 workstation was used to solve the Navier-Stokes equations for low Reynolds number (Re) flow in a cylindrical tube with one or more spheres fixed to the vessel wall. A geometrical model is constructed, over which the equations of flow are solved at discrete points. The model consists of a sphere sitting on a neck, the diameter of which is one-half the diameter of the sphere, connecting the cylindrical tube wall and the sphere surface. The neck prevents a degenerate point where the sphere and cylinder contact. This neck is blocked to flow and is treated as part of the sphere. Decreasing the diameter of the neck does not significantly change the solution, as judged by the pressure drop across the sphere, the length of the disturbed flow region, and the total fluid drag force on the sphere. Whenever possible, we take advantage of symmetry planes in the geometry. For example, for a single sphere adherent to a cylindrical vessel, only one-half of the three-dimensional geometry needs to be gridded. The complete solution is obtained by duplicating and reflecting the partial solution about the plane of symmetry. Gridding half the geometry allows either half the number of cells to be used, cutting down on computational time, or the same number of cells that would be used in the complete geometry can be used in the half-geometry, resulting in a more detailed solution. The validity of the computational solutions was verified by comparing the results of the computations to experimentally obtained results for pressure drop across a single sphere, length of the perturbed flow region, and fluid force on the sphere (Chapman and Cokelet, 1997).

The calculations were done in three dimensions, and the criterion for convergence was at least a five order of magnitude reduction in the total residuals. The number of grid cells was increased until a further increase in cell number did not change the solution as determined by the flow profile in the region of the sphere, as well as the force exerted by the flow on the adherent sphere and vessel wall in the sphere region. Typically, the domain over which the Navier-Stokes equations were solved consisted of fewer than 60,000 cell volumes, with a run time on the order of 12 h.

The boundary conditions were zero velocity on all surfaces, and either a parabolic inlet velocity or a uniform inlet velocity with an entrance length sufficient to establish Poiseuillian flow before flow reached the perturbed flow region near a sphere. The blood is modeled as a Newtonian fluid with appropriate mean velocity, density, and viscosity, so that the Reynolds number is 0.01.

Two main geometries of multiple sphere adhesion examined in this study are shown in Fig. 1. These geometries are referred to as *aligned* and *opposite* configurations. This is somewhat confusing, in that for both cases the spheres are aligned. However, the aligned configuration refers to the situation in which the spheres are adherent on the same side of the vessel, whereas for the opposite configuration the spheres are adherent on opposite sides of the vessel wall. For both cases we examine the pressure drop across, and drag forces on, multiple leukocytes as a function of the separation distance between the spheres. The separation distance, d_s, is always the distance between sphere centers.

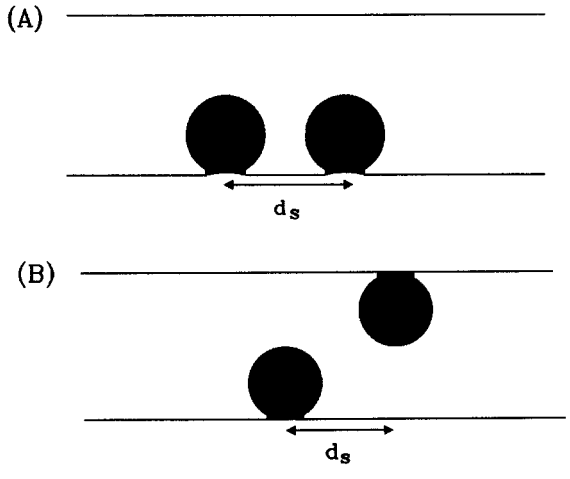

FIGURE 1 The two major geometries examined are (*A*) aligned and (*B*) opposite configurations. This figure shows the geometry for a cut down the center of the vessel and the sphere, for two adherent spheres. The separation distance (d_s) is defined as the length between the centers of adjacent spheres.

We have developed dimensionless correlations to calculate the drag force on a single adherent leukocyte (Chapman and Cokelet, 1996) and the pressure drop across the flow region disturbed by the adherent leukocyte (Chapman and Cokelet, 1997), based on computational and experimental methods. The correlation for calculating the drag force is

$$C_d * \mathrm{Re} = \left(8.15 - \frac{7.52}{\ln(d/D)}\right)^2 \quad (1)$$

The correlation for calculating the pressure drop across one sphere is

$$f * \mathrm{Re} = \exp\left(2.877 + 4.630\left(\frac{d}{D}\right)^4\right) \quad (2)$$

where C_d is the drag coefficient:

$$C_d = \frac{F_o}{(1/2)\rho A V^2} \quad (3)$$

Re is the Reynolds number:

$$\mathrm{Re} = \frac{\rho V D}{\eta} \quad (4)$$

so that

$$F_o = \frac{\pi(C_d * \mathrm{Re}) d^2 V \eta}{8D} \quad (5)$$

f is the Fanning friction factor:

$$f = \frac{\Delta P' D}{2L_d \rho V^2} \quad (6)$$

so that

$$\Delta P' = \frac{2(f * \mathrm{Re}) L_d V \eta}{D^2} \quad (7)$$

d/D is the sphere-to-tube diameter ratio; F_o is the fluid force on an isolated sphere; ρ is fluid density; A is the cross-sectional area of the sphere; V is the average fluid velocity ($\equiv$ volumetric flow rate/cross-sectional area of unobstructed tube); D is the tube diameter; η is the fluid viscosity; d is the sphere diameter; $\Delta P'$ is the pressure drop across a disturbed flow region (one sphere); and L_d is the length of the disturbed flow region (one sphere).

To calculate the force on an adherent leukocyte, the ratio of leukocyte diameter to vessel diameter (d/D) is required. C_d * Re is calculated from Eq. 1, using the appropriate measured d/D ratio. This value of C_d * Re, along with the fluid viscosity and average velocity, is used to calculate the fluid drag force on the leukocyte from Eq. 5. A similar procedure is conducted to determine the pressure drop in a vessel with an adherent leukocyte, using the correlation given by Eq. 2 to determine f * Re, and then Eq. 7 to calculate the pressure drop. Equations 1 and 2 are valid for a Newtonian fluid with $\mathrm{Re} < 1$ and $0.10 \leq d/D \leq 0.83$. The flow in the microcirculation has a low Re, and for an 8-μm-diameter human neutrophil, the d/D range examined corresponds to vessels whose diameters are between 9.6 μm and 80 μm. Previous work suggests that RBCs may influence Eqs. 1 and 2 for $d/D > 0.33$, which corresponds to vessels smaller than 24 μm for an 8-μm leukocyte (Chapman and Cokelet, 1996, 1997).

When multiple spheres interact, the force on one of the interacting spheres (F_s) is normalized to the force on a single isolated sphere (F_o). This is equivalent to normalizing the dimensionless group for one of the interacting spheres, $(C_d * \mathrm{Re})_s$, by C_d * Re (given in Eq. 1). The situation is more complicated when the pressure drop across multiple leukocytes is calculated, because the nature of the disturbed flow region varies with the number of adherent spheres. Therefore the pressure drop (or f * Re) across multiple spheres is not normalized to the pressure drop (or f * Re) across one sphere. Using Eqs. 1 and 5 to calculate the force on an adherent leukocyte interacting with other adherent leukocytes is straightforward. However, further explanation is required on how the f * Re correlations are used to calculate the flow resistance, or pressure drops, in blood vessels.

Increased resistance to flow in a vessel generated by adherent leukocytes

All spheres act independently

Fig. 2 illustrates the simplest situation, in which the spheres are spaced sufficiently far apart that they act independently. L is the vessel length, L_d is the perturbed flow region per sphere, ΔP_s is the total pressure drop, and $\Delta P'$ is the pressure drop across each sphere's disturbed flow region. With the restriction that the spheres cannot interact, there is a maximum number of spheres, per unit length, that can be contained within the vessel. A previous study, in which disturbed flow was defined as a 1% deviation from undisturbed flow, determined the length of the disturbed flow as a function of d/D for $0.10 \leq d/D \leq 0.83$ (Chapman and

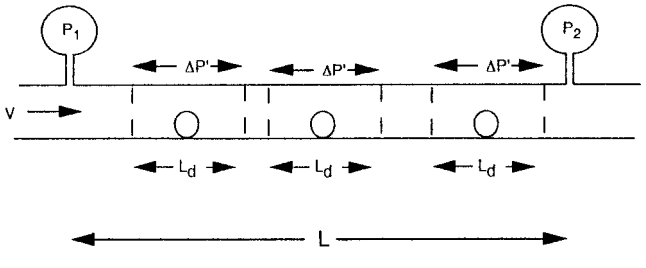

FIGURE 2 For multiple adherent spheres in a vessel, the flow can be broken into two regions. There is a region where the flow is disturbed by the presence on an adherent sphere, and there may be regions where the flow is undisturbed. Thus, in a vessel of length L and n adherent spheres, the total pressure drop is n times the pressure drop across the disturbed flow length of one sphere plus the pressure drop in the remainder of the vessel ($L - nL_d$).

Cokelet, 1997):

$$L_d = 2D[-0.115 + 6.216(d/D) - 11.688(d/D)^2 + 11.044(d/D)^3 - 4.018(d/D)^4] \quad (8)$$

The total pressure drop for the situation given in Fig. 2 can be calculated by separating the vessel into disturbed flow regions and undisturbed flow regions. The pressure drop across each adherent sphere is determined from Eq. 7. For the undisturbed flow region, $f^* \mathrm{Re} = 16$ (Shah and London, 1978), so that the total pressure drop in the undisturbed flow regions is

$$\Delta P_u = 32(L - nL_d)V\eta/D^2$$

Therefore, the total pressure drop over the vessel length L is

$$\begin{aligned}\Delta P_s &= n\Delta P' + \Delta P_u \\ &= 2n(f^* \mathrm{Re})L_d V\eta/D^2 + 32(L - nL_d)V\eta/D^2 \\ &= 2V\eta/D^2\{n(f^* \mathrm{Re})L_d + 16(L - nL_d)\}\end{aligned}$$

where f^* Re is calculated from Eq. 2.

If no adherent spheres are present, the pressure drop over the total length L is

$$\Delta P_o = 32LV\eta/D^2$$

The resistance generated by the adherent spheres, normalized to the resistance when no spheres are present, is

$$\begin{aligned}R_s/R_o &= \Delta P_s/\Delta P_o \\ &= \{2V\eta/D^2[16(L - nL_d) + n(f^* \mathrm{Re})L_d]\}/\{32LV\eta/D^2\} \\ &= \{16(L - nL_d) + n(f^* \mathrm{Re})L_d\}/(16L) \quad (9)\end{aligned}$$

All spheres interact without intermingled undisturbed regions

If the spheres are spaced close enough together such that they interact and there are no undisturbed flow regions, the solution is more complicated. The adherent spheres can vary in the angular position they have relative to each other, in the separation distance between adjacent spheres and in the total number of interacting adherent spheres. The results of the present study, in which the pressure drop across various geometric configurations for multiple adherent spheres is examined, must be utilized.

The pressure drop across multiple interacting spheres is used to define $(f^* \mathrm{Re})_{ms}$. From a similar development shown for Eq. 9, the resistance ratio for interacting spheres (where the entire vessel length L is in perturbed flow) is

$$R_{ms}/R_o = (f^* \mathrm{Re})_{ms}/16 \quad (10)$$

We have determined $(f^* \mathrm{Re})_{ms}$ for various numbers of adherent spheres, variable spacing, and opposite and aligned configurations.

Resistance increase for combination of interacting and noninteracting spheres

The most complicated situation is that in which spheres are spaced such that some spheres interact and others are independent, and there are also regions where the flow is undisturbed. To develop a generalized equation, we break the pressure drop in the vessel into three components:

1. undisturbed region
2. disturbed by independently acting spheres
3. disturbed by interacting spheres

Components 1 and 2 are contained in Eq. 9, and component 3 is contained in Eq. 10. Of course, component 3 is further divided if there are different regions within the vessel where the geometry and/or spacing of the spheres varies. However, as the results will show, certain simplifications can be made. The generalized equation for calculating the resistance increase for a vessel of length L is then

$$R_s/R_o = [16(L - nL_d) + n(f^* \mathrm{Re})L_d + \sum\{(f^* \mathrm{Re})_i L_i\}/(16L) \quad (11)$$

where L_i is the perturbed flow length, for a given region of multiple, interacting spheres, whose product with $(f^* \mathrm{Re})_i$ is summed over all multiple, interacting regions. The first term on the right-hand side of Eq. 11 represents the undisturbed flow regions, the second the regions disturbed by single (noninteracting) spheres, and the third term represents all flow regions of multiple, interacting spheres. The summation for the last term in Eq. 11 is required if there are multiple regions of multiple, interacting spheres where the spacing and/or orientations of the spheres are such that the ΔP contributions from each region are different.

RESULTS

Two spheres in a vessel

Initial studies were conducted to determine the drag force and pressure drop on one of two interacting spheres as a function of separation distance between the two spheres. (Because for steady, incompressible, constant-viscosity, low Reynolds number flows, the equations of motion are linear and time does not explicitly enter into their solutions, the drag force and pressure drops for each of the spheres are equal.) Fig. 3 shows the dependence of the drag force on the separation distance for spheres aligned and opposite one another. For two interacting spheres, when the spheres are on opposite sides of the vessel axis, the drag force on one of the spheres (F_s) is greater than that for a single isolated sphere (F_o), and is a function of sphere separation distance (d_s) and the sphere diameter to vessel diameter ratio (d/D). When the second sphere is directly downstream from the first, $F_s/F_o \leq 1.0$, and F_s/F_o varies with d_s and d/D. The maximum increase in the drag on a sphere occurs when two spheres are adherent opposite each other, with minimal spacing (d_s/D) between the two spheres. The decrease in force is at maximum when the spheres are aligned and

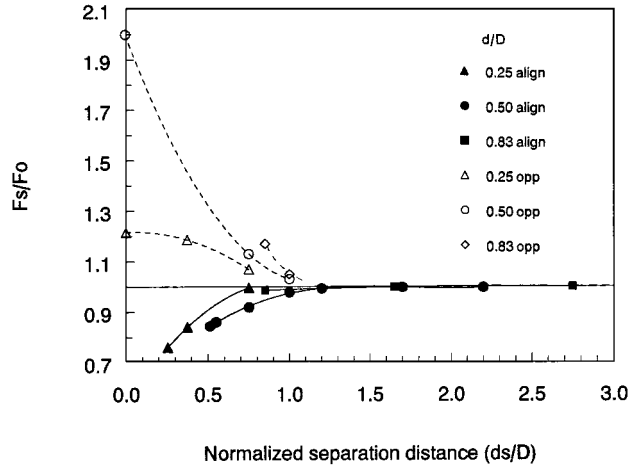

FIGURE 3 The drag force on one of a pair of adherent spheres (F_s), normalized with the drag force on an isolated, adherent sphere (F_o), as a function of separation and orientation. Shown are three d/D ratios (0.25, 0.50, and 0.83) with two orientations, aligned (*solid symbols*) and opposite (*open symbols*).

touching one another ($d_s/D = d/D$). As the separation distance between the spheres increases, the drag force on each of the spheres approaches the drag experienced by an independent adherent sphere. Fig. 3 shows that when spheres are separated by more than 1.2 vessel diameters, the correlation for the drag on a single isolated adherent sphere can be used to calculate the drag force on each of the two adherent spheres.

A similar presentation is shown in Fig. 4 for the relative flow resistance across two adherent spheres, normalized to the flow resistance when no adherent spheres are present. (This is equivalent to the relative pressure drop for a constant flow rate.) A striking difference between Figs. 3 and 4 is the relatively small change in pressure drop, compared to the change in drag force, when a second sphere is aligned with the first. There is also little effect of separation distance on the pressure drop when the spheres are aligned. This suggests that sphere spacing will have little affect on $(f * \mathrm{Re})_{ms}$ and $(f * \mathrm{Re})_i$, given by Eqs. 10 and 11. However, when the spheres adhere on opposite sides of the vessel, there is a larger effect on the pressure drop. For $d/D = 0.5$, the pressure drop across the disturbed flow region almost doubles. As the separation distance between the two spheres increases, the $f * \mathrm{Re}$ value approaches the value for one isolated sphere. For $d/D = 0.25$, there is comparatively little increase in the pressure drop when additional spheres are aligned with an initial adherent sphere. We would expect the maximum resistance increase to occur if our spheres were replaced by an eccentric solid cylinder running the entire length of the vessel wall. For the eccentric cylinders, where the ratio of cylinder diameter to vessel diameter is 0.25, 0.50, and 0.83, ratio of the resistance when spheres are present to the resistance when no spheres are present is 1.30, 2.56, and 15.1, respectively.

More than two spheres in a vessel

To develop generalized correlations to calculate drag forces on, and pressure drops across, any number of adherent leukocytes, we must examine the situation in which there are at least three interacting adherent spheres. For three or more interacting spheres in a line, F_s/F_o for the interior spheres is less than that for the end spheres. The simplest situation is shown in Fig. 5, where the drag force (for three

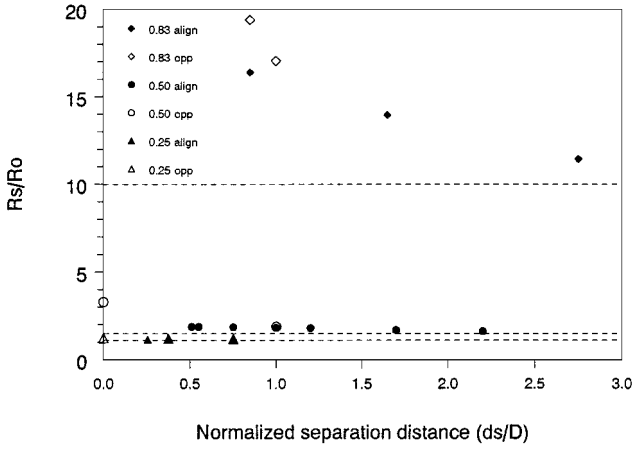

FIGURE 4 A plot of the pressure drop across the disturbed flow region, normalized to the pressure drop when no adherent spheres are present (equivalent to relative resistance R_s/R_o, for a constant flow rate), generated by two adherent spheres as a function of separation and orientation. The symbols represent the d/D ratio; filled and open symbols represent aligned and opposite configurations, respectively. The dashed lines are the R_s/R_o values for a single adherent sphere, with the smallest R_s/R_o value corresponding to $d/D = 0.25$, the middle to $d/D = 0.50$, and the largest to $d/D = 0.83$.

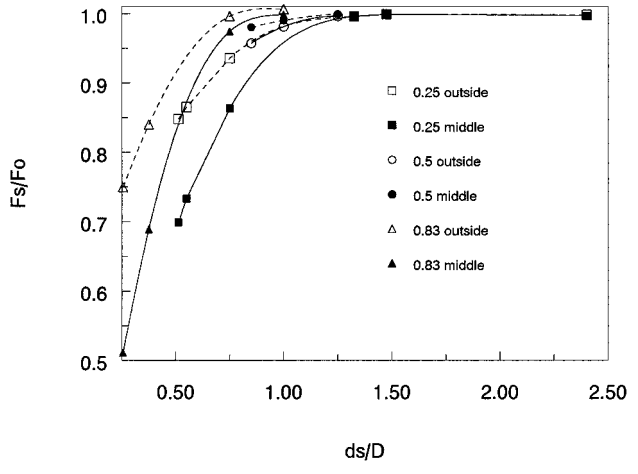

FIGURE 5 The drag force on one of three adherent spheres (F_s), normalized to the drag force on an isolated sphere (F_o), as a function of separation distance. In this example the separation distance between the first and second spheres equals the separation distance between the second and third spheres. Each symbol represents a d/D ratio, and the open and closed symbols refer to the outside (upstream and downstream) and middle spheres, respectively.

d/D ratios) is shown as a function of separation distance for three evenly spaced and aligned spheres. As the spheres approach each other, the drag on each sphere increasingly decreases. However, the drag on the middle sphere experiences a larger decrease, which is more pronounced for smaller d/D ratios. This observation has important consequences when leukocyte adhesion in vivo is considered. For any number of equally spaced spheres, the correlation from Fig. 5 can be used to calculate the force on each sphere. This is demonstrated in Fig. 6 for $d/D = 0.50$ and $d_s = 0.51D$. Regardless of the number of aligned spheres, there is only one of two possible drag forces on a given sphere. The edge spheres experience larger drag forces, whereas any spheres in the middle experience a comparatively smaller drag force (of essentially the same magnitude).

Fig. 7 shows the drag force on each of three unevenly spaced adherent spheres where $d/D = 0.25$. The spatial arrangement is varied by keeping constant the distance between the first and last spheres and varying the position of the middle sphere. The drag force on the interior sphere is not sensitive to the spatial arrangement of the three spheres. When the spheres are evenly spaced ($d_{12}/(d_{12} + d_{23}) = 0.5$), the force on the spheres can be obtained from Fig. 5. As the middle sphere is moved toward the first sphere, the force on the first sphere decreases, and the force on the third sphere increases. However, the force on the middle sphere remains relatively constant. There is a symmetry line at $d_{12}/(d_{12} + d_{23}) = 0.5$, so that the trend for $d_{12}/(d_{12} + d_{23}) > 0.5$ can be obtained from the data shown in Fig. 7. In addition, the pressure drop across the aligned spheres given in Fig. 7 is independent of the spatial arrangement (data not shown). This suggests that for an aligned geometry, the sphere spacing for multiple, interacting spheres is not a very sensitive parameter when ΔP is calculated.

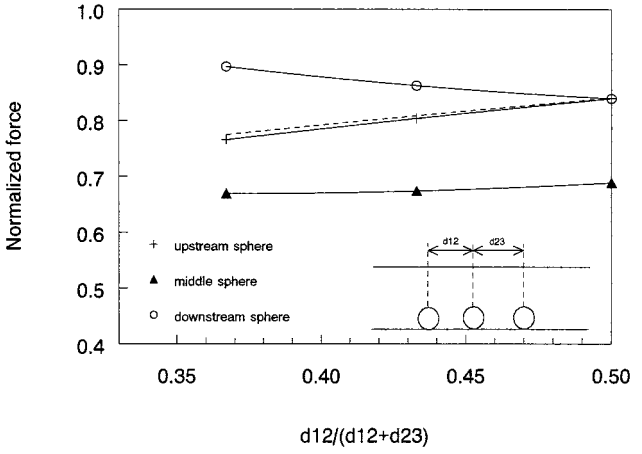

FIGURE 7 The normalized drag force on each of three aligned adherent spheres for $d/D = 0.25$ as a function of spatial arrangement. The spatial arrangement is defined as the fractional position of the middle sphere relative to the first sphere. The dashed line is the drag force correlation obtained for two interacting spheres, obtained from Fig. 3. In this example, the distance between the centers of the two end spheres is $0.75D$. If a larger separation is used, the correlation degenerates into the drag correlation for an isolated sphere and the two-sphere correlation (Fig. 3) as the middle sphere deviates from its central position toward an edge sphere.

An example of the relative importance of sphere number versus sphere spacing in the calculation of ΔP is given in Fig. 8. For both d/D ratios, varying d_s/D has little effect on the pressure drop in the vessel. This suggests that the spacing of aligned, interacting spheres has relatively little influence on the pressure drop in the vessel.

Fig. 8 suggests that a more important parameter when determining the resistance increase within a vessel is the number of adherent spheres contained within a blood vessel. To calculate the relative resistance increase in a blood

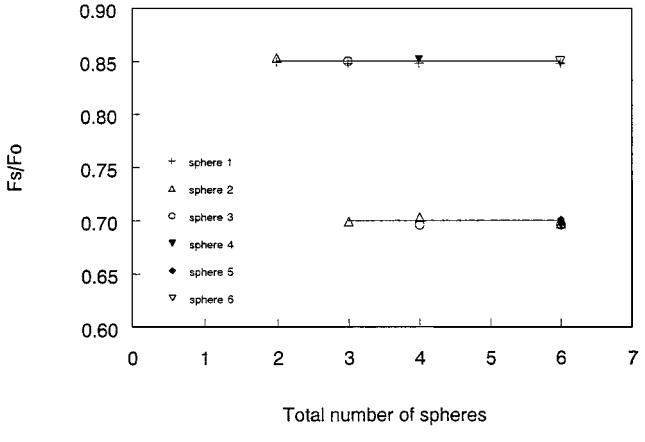

FIGURE 6 The normalized drag force for various numbers of aligned adherent spheres, with $d/D = 0.50$ and $d_s = 0.51D$. The sphere position is given in the legend, where sphere 1 is the upstream sphere, progressing in the downstream position with increasing sphere number. Regardless of the number of spheres present, the spheres experience only one of two possible drag forces, depending on their position. For example, when four spheres are present, the drag force on the end spheres (1 and 4) is $0.85F_o$, and the drag force on the middle spheres (2 and 3) is $0.70F_o$.

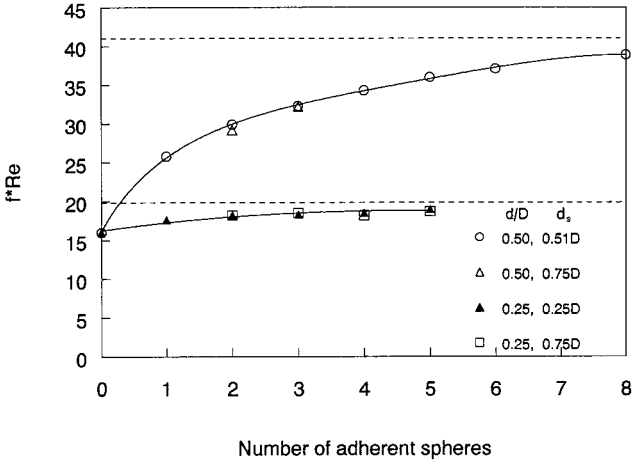

FIGURE 8 The correlation needed to calculate the pressure drop as a function of the number of aligned, adherent spheres. d/D ratios of 0.5 and 0.25 are shown, each with two separate sphere spacings normalized to the vessel diameter. The dashed line is the limit when all of the spheres are replaced by a solid cylinder.

vessel, increasing numbers of spherical leukocytes (8 μm in diameter) were added in an aligned configuration in a 100-μm-long, 16-μm-diameter vessel. This is shown in Fig. 9, along with the relative resistance when the spheres are replaced by a solid cylinder running the entire length of the vessel wall, unlike our spheres, which were not allowed to be within $L_d/2$ of the vessel entrance or exit.

DISCUSSION

This study addresses the increased flow resistance in a blood vessel generated by adherent leukocytes and the change in the adhesive force required for leukocytes to remain adherent to the blood vessel wall. Before these questions are addressed, some limitations of the study should be discussed.

We modeled blood as a Newtonian fluid and neglected the presence of red blood cells (RBCs). RBCs affect the fluid properties by blunting the velocity profile in postcapillary vessels and changing the effective viscosity of the fluid. Previous work suggests (for an 8-μm-diameter leukocyte) that as long as the change in viscosity is accounted for, RBCs do not affect our drag correlation if the vessel diameter is larger than 24 μm (Chapman and Cokelet, 1996), and they do not affect our pressure correlation if the diameter is greater than 16 μm (Chapman and Cokelet, 1997). Therefore, our results should be applied with care for blood vessels smaller than ~24 μm. Studies of in vitro flows in parallel plate flow channels have shown that red cells do affect the transverse motion of leukocytes and would therefore be expected to increase the normal force between an adherent leukocyte and the vessel wall (Melder et al., 1995)

The geometry was simplified by modeling the leukocyte as a rigid sphere and the blood vessel as a straight, smooth cylinder. Blood vessels are not smooth, cylindrical tubes, but can follow a tortuous path and have endothelial cells lining the vessel wall whose nuclei bulge into the vessel (Barbee et al., 1994). In addition, leukocytes are not rigid spheres, but can deform once they adhere to the venular endothelium (Shen and Lipowsky, 1997). However, low Re flow tends to minimize the effects of the vessel roughness, bends, and WBC shape by rapidly reestablishing flow profiles. The shape of the leukocyte is less important than the cross-sectional area presented to flow for small d/D ratios. However, the drag force on, and pressure drop across, the leukocyte become more sensitive to the leukocyte's shape as the vessel size decreases.

Increase in flow resistance

In postcapillary venules, various numbers of adherent leukocytes are observed. The number of adherent leukocytes per vessel length can vary greatly, depending on the tissue state, anywhere between 0 and 11 per 100 μm (House and Lipowsky, 1987). We can use the results from this study to predict how much the pressure drop must increase to keep flow constant through the blood vessel for various numbers of adherent leukocytes.

The simplest situation in calculating the resistance increase occurs when all of the adherent leukocytes are spaced far enough apart that they act as independent particles. With this constraint, Eq. 9 can be used to calculate the relative resistance increase, in vessels of various sizes, generated by an 8 μm leukocyte. Fig. 10 is an example of this for L = 100 μm. The 1 WBC curve is the resistance when only one leukocyte is adherent and is calculated as

$$\left(\frac{R_s}{R_o}\right)_{1\ \mathrm{WBC}} = \frac{16(100 - L_d) + (f * \mathrm{Re})L_d}{1600}$$

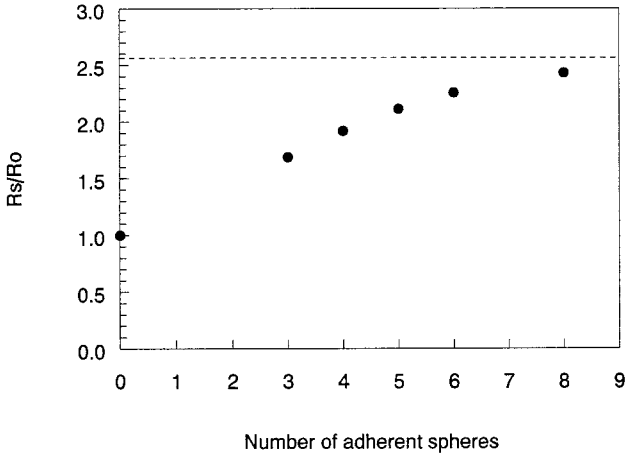

FIGURE 9 Resistance for d/D = 0.50 (8-μm leukocyte in a 16-μm vessel), normalized to the resistance without adherent spheres for various numbers of adherent spheres. The dashed line is the relative resistance when all of the spheres are replaced by a solid cylinder that runs the length of the vessel along the wall.

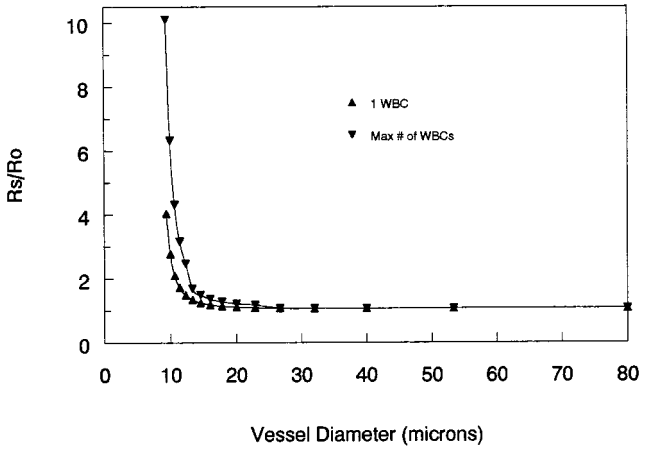

FIGURE 10 Relative resistance increase generated by independent adherent leukocytes in a 100-μm length of vessels of various diameters. The 1 WBC curve is the resistance generated when only one leukocyte is adherent. The max curve is obtained by placing the maximum number of independently acting leukocytes in the vessels. For $D \geq 25$, one leukocyte at most can be placed in the vessel; a second leukocyte results in interactions.

f^* Re and L_d are calculated from Eqs. 2 and 8, respectively. The second curve is the relative resistance increase when the maximum number of leukocytes are adherent in the vessel. The maximum number of adherent leukocytes is L/L_d, rounded down to the next smallest integer, because a fraction of a leukocyte is meaningless. For smaller d/D ratios (or larger diameter vessels), no more than one leukocyte may adhere in the vessel without violating our strict noninteraction requirement. We conclude from Fig. 10 that the resistance to flow cannot significantly increase in vessels more than 20 μm in diameter when leukocytes adhere far enough apart such that they act independently. It has been reported that without an activating stimulus, very few leukocytes adhere to the vessel wall (Jones et al., 1995). However, as the vessel diameter decreases from 20 μm to 10 μm, the resistance to flow increases dramatically, both for one adherent leukocyte and multiple, independently adherent leukocytes. One adherent leukocyte in a 10-μm-diameter vessel results in approximately a fourfold increase in the flow resistance. If the maximum number of independent leukocytes adhere in this size vessel, there is a 10-fold increase in the vessel's resistance.

However, the flow resistance can increase to values much greater than those given in Fig. 10 if the leukocytes can adhere in proximity to others. Fig. 11 shows how the resistance changes with the number of adherent leukocytes, per 100 μm length of vessel, for the three d/D ratios examined in this study. The filled symbols are calculated using Eq. 11. As mentioned when we described Fig. 9, it only takes three aligned 8-μm leukocytes in a 9.8-μm-diameter vessel to raise the flow resistance 10-fold. The filled symbols in Fig. 11 are minimum resistance increases because the leukocytes are aligned, the most favorable condition for a minimum resistance increase. If leukocytes adhere in the opposite configuration, with no separation distance between a pair of leukocytes, the resistance can significantly increase, as shown by the open symbols. There is an intermediate increase in the resistance (for all d/D examined), when spheres alternate on the side of the vessel wall to which they adhere.

Analytical solutions are available for the situation in which the aligned leukocytes are replaced by a solid cylinder that runs along the length of the vessel on the wall. Based on table 100 in Shah and London (1978), R_s/R_o = 2.56 and 1.30 for d/D = 0.50 and 0.25, respectively. These values compare favorably to the maximum resistance increase generated by aligned adherent spheres for d/D = 0.50 and 0.25 in Fig. 11.

Few published studies that examined the pressure drop across adherent spheres are available for comparison. A large-scale model, where d/D = 0.4, determined that R_s/R_o = 1.7 for 10 aligned adherent spheres (Bagge et al., 1986). We can use our correlations to predict a resistance increase based on the experimental conditions used by Bagge et al. From data such as those given in Figs. 8 and 9, we can plot the relative resistance increase for 10 adherent spheres as a function of d/D. Fig. 12 shows this plot for the three multiple d/D ratios examined in this study. From the best-fit curve, our data predict that for 10 aligned adherent spheres (d/D = 0.4), R_s/R_o = 1.62, in agreement with their experimentally obtained value of 1.7. Also shown in Fig. 12, by the dashed line, is the relative resistance generated if the spheres are replaced by a solid cylinder running the length of the vessel wall.

When the spheres are aligned opposite each other in two rows, so that there are 20 adherent spheres, Bagge et al. found that R_s/R_o = 2.3. For comparison, our CFD results indicate that R_s/R_o increased from 1.3 to 1.8 for d/D = 0.25 when going from the aligned (10 spheres) to the opposite (20 spheres) configuration.

Eriksson and Robson (1977) conducted a mathematical treatment to calculate the resistance increase generated by

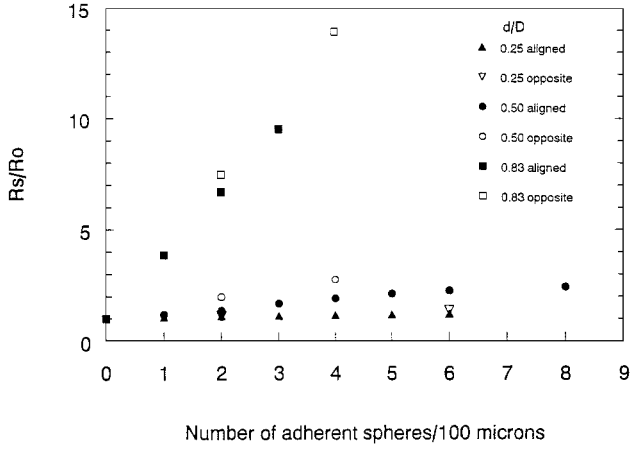

FIGURE 11 Relative resistance increase generated by any number of adherent leukocytes for three vessels of different diameters (D = 32 μm, 16 μm, and 9.8 μm, based on a leukocyte diameter of 8 μm). The closed symbols represent the case in which all leukocytes are aligned, and the open symbols are a worst-case resistance increase when cells are aligned opposite one another.

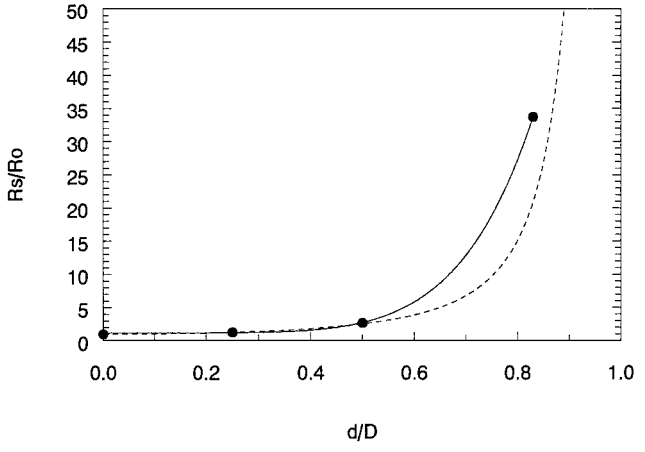

FIGURE 12 The resistance across 10 aligned adherent spheres, divided by the resistance without adherent spheres, is plotted as a function of d/D. The dashed line is the relative resistance for a cylinder running the length of the vessel wall.

various configurations of adherent leukocytes. They used the classic Poiseuillian relationship to estimate resistance increases in 25.2-μm-diameter ($d/D = 0.32$) postburn venules. Using a hydraulic diameter in Poiseuille's law, they estimated that $R_s/R_o = 3.6$, for 16 adherent leukocytes aligned such that they are all touching, in a 200-μm length of vessel. This resistance increase is higher than our correlations predict. For $d/D = 0.5$, $L = 200$ μm, $L_D = 188.5$, we would calculate, from Eq. 11,

$$R_s/R_o = [16(11.5) + 52.9(188.5)]/(16 * 200) = 3.2$$

There are some in vivo data for which the pressure drop was measured in vessels with various numbers of adherent leukocytes (Lipowsky et al., 1980; House and Lipowsky, 1987). In a 42-μm vessel ($d/D = 0.2$ if $d = 8$ μm), Lipowsky et al. (1980) reported that $R_s/R_o = 1.74$ for an average of six adherent leukocytes per 100 μm. This is a larger resistance increase than we would predict from our correlations. If the leukocytes were aligned, we would predict that $R_s/R_o = 1.21$, and if they were in an opposite configuration, $R_s/R_o = 1.38$. In a subsequent study (House and Lipowsky, 1987), R_s/R_o was determined to be 1.81 in a 40-μm vessel, with 11.4 leukocytes adherent per 100 μm vessel length. Again, this resistance increase is higher than the resistance increase that would be calculated by the present study ($R_s/R_o = 1.55$ in opposite configuration). The difference in the resistance increase could be due to such factors as the uncertainty in the in vivo d/D ratio (we assumed that $d = 8$ μm, but certain leukocyte types can have larger diameters); the different geometry of adhesion, so that there is an even larger increase in the pressure drop; noncircularity of the vessel cross sections; and/or the presence of RBCs.

Drag force on interacting leukocytes

Figs. 3 and 5 show the importance of neighboring leukocytes on the drag force experienced by an adherent leukocyte. When leukocytes are close enough so that their flow disturbances interact, the drag force decreases or increases, depending on the geometry of adhesion. This study focused on the aligned and opposite geometries because of computational constraints. However, a preliminary study indicates that the relative angle of adhesion for interacting spheres influences the drag force on an adherent sphere. For two adherent spheres with $d/D = 0.25$, $d_s = 0$, and a relative adhesion angle of 90°, the drag force on each sphere was $1.36F_o$ compared to $1.22F_o$, and the pressure drop across the disturbed flow region was only slightly lower than when the angle was 180°. This suggests that for $d/D < 0.5$, the largest drag force may occur for relative geometries other than an opposite adhesion (angle $\neq$ 180°).

An interesting observation is that the relative change in drag force is sensitive to the vessel diameter. For smaller diameter vessels, the relative decrease in drag force is more pronounced than in larger vessels (Figs. 3 and 5). The larger decrease in the normalized drag force in small vessels arises from the stress distribution over the surface of the leukocyte. Fig. 13 shows the stress distribution along the surface of an adherent sphere, on the circle generated by the plane parallel to the flow and passing through the sphere center, for three d/D ratios. For larger d/D ratios, most of the force on the leukocyte arises from the narrow gap region between the sphere and vessel wall for a central cut down the center of the sphere and vessel. When subsequent leukocytes adhere, there is a decrease in the stress on the upstream and downstream portions of the sphere edge, whereas the stress in the narrow gap region, centered around an angle of 180°, does not change significantly. As a result, there is a larger relative decrease in the drag force with multiple adherent spheres in the larger size vessels. The stress distribution on a leukocyte will change, of course, as the cell deforms from the spherical shape.

The variations in the drag force exerted on interacting leukocytes is important to include in models addressing the biophysics of receptor-ligand interactions for cells adhering to the walls of blood vessels. Models of cell adhesion are an important aid in understanding receptor-ligand interactions. One parameter required by these models is the fluid drag exerted by the passage of fluid over the adherent leukocyte. Solutions are available for the drag force past a sphere adherent to a flat surface [(Goldman et al., 1967a,b), and models of cell adhesion to flat surfaces have been developed (Bell, 1978; Hammer and Lauffenburger, 1987; Cozens-Roberts et al., 1990). However, previous to our studies, solutions for the drag force pertinent for flow past an adherent leukocyte in postcapillary size vessels were limited (Schmid-Schönbein et al., 1975; House and Lipowsky, 1988). With the development of a correlation to calculate the drag force on multiple adherent leukocytes in vessels of various sizes, models can be extended to adherent cells in cylindrical vessels to determine information such as the minimum number of bonds required to firmly arrest a leukocyte.

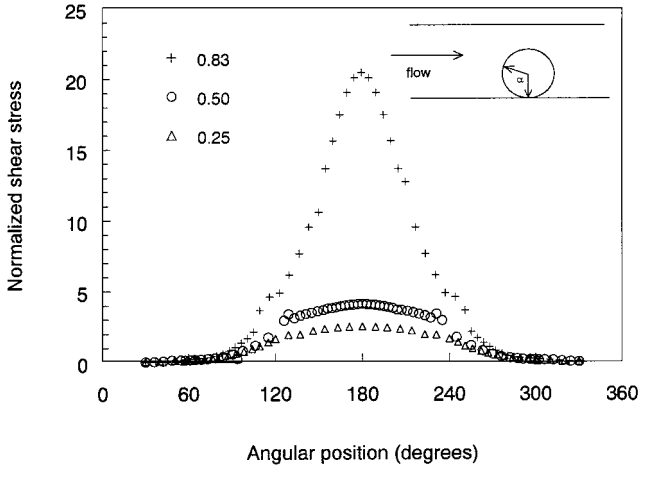

FIGURE 13 Shear stress, normalized to the wall stress far from the adherent sphere, on the surface of the sphere as a function of angular position for three d/D ratios.

This study demonstrates how multiple adherent leukocytes in close proximity can affect the drag force exerted on an adherent leukocyte. There must be sufficient integrin-mediated interactions between the surface of the leukocyte and endothelial cells to withstand the drag force acting to sweep the leukocytes along the vessel wall. If the level of receptor (or ligand) expression is such that there is a small difference between the adhesive and dispersal forces, there will be preferred locations of adhesion once an initial leukocyte adheres. These locations will be directly upstream or downstream from the initial adherent leukocyte. However, there are also areas opposite the adherent leukocyte where fewer leukocytes will adhere because of elevated forces acting to sweep leukocytes along the vessel wall. We have shown that the drag force can vary substantially, from half to twice the force on an isolated adherent leukocyte. Of course, if receptor (or ligand) expression is nonuniform over the endothelium, then both hemodynamics and receptor levels will determine where a leukocyte will adhere.

Another important physiological effect of multiple adherent leukocytes is the impact on convective transport of any mediators/chemokines released by leukocytes, endothelial cells, or infected cells in these areas. Similar to 2-D computations of concentration gradients generated by thrombi (Folie and McIntire, 1989), areas immediately upstream and downstream of adherent leukocytes will experience a build-up of any substances released to that area. The build-up will be greater between aligned and closely spaced leukocytes, where stagnant flow is even more prominent. This could lead to higher local chemoattractant concentrations and/or receptor activation on the endothelial surface, and further leukocyte recruitment. This could be an additional mechanism for confining leukocyte adhesion to precise locations within a blood vessel during tissue infection and damage.

This work was supported by U.S. Public Health Service–National Institutes of Health grant HL18208.

REFERENCES

Bagge, U., A. Blixt, and M. Braide. 1986. Macromodel experiments on the effect of wall-adhering white cells on flow resistance. *Clin. Hemorheol.* 6:365–372.

Barbee, K. A., P. F. Davies, and R. Lal. 1994. Shear stress-induced reorganization of the surface topography of living endothelial cells imaged by atomic force microscopy. *Circ. Res.* 74:163–171.

Bell, G. I. 1978. Models for the specific adhesion of cells to cells. *Science.* 200:618–627.

Chapman, G., and G. Cokelet. 1996. Model studies of leukocyte-endothelium-blood interactions. I. The fluid drag force on the adherent leukocyte. *Biorheology.* 33:119–138.

Chapman, G. B., and G. R. Cokelet. 1997. Model studies of leukocyte-endothelium-blood interactions. II. Hemodynamic impact of leukocytes adherent to the wall of post-capillary vessels. *Biorheology.* 34:37–56.

Cozens-Roberts, C., J. A. Quinn, and D. A. Lauffenburger. 1990. Receptor-mediated adhesion phenomena. Model studies with the radial-flow detachment assay. *Biophys. J.* 58:107–125.

Eriksson, E., and M. C. Robson. 1977. New pathophysiological mechanism explaining post-burn oedema. *Burns.* 4:153–156.

Folie, B. J., and L. V. McIntire. 1989. Mathematical analysis of mural thrombogenesis. *Biophys. J.* 56:1121–1141.

Goldman, A. J., R. G. Cox, and H. Brenner. 1967a. Slow viscous motion of a sphere parallel to a plane wall. I. Motion through a quiescent fluid. *Chem. Eng. Sci.* 22:637–651.

Goldman, A. J., R. G. Cox, and H. Brenner. 1967b. Slow viscous motion of a sphere parallel to a plane wall. II. Couette flow. *Chem. Eng. Sci.* 22:653–660.

Hammer, D. A., and D. A. Lauffenburger. 1987. A dynamical model for receptor-mediated cell adhesion to surfaces. *Biophys. J.* 52:475–487.

House, S. D., and H. H. Lipowsky. 1987. Leukocyte-endothelium adhesion: microhemodynamics in mesentery of the cat. *Microvasc. Res.* 34:361–379.

House, S. D., and H. H. Lipowsky. 1988. In vivo determination of the force leukocyte-endothelium adhesion in the mesenteric microvasculature of the cat. *Circ. Res.* 63:658–668.

Jones, D. A., C. W. Smith, and L. V. McIntire. 1995. Effects of fluid shear stress on leukocyte adhesion to endothelial cells. *In* Physiology and Pathophysiology of Leukocyte Adhesion. Oxford University Press, New York. 148–168.

Lipowsky, H. H., S. Usami, and S. Chien. 1980. In vivo measurements of "apparent viscosity" and microvessel hematocrit in the mesentery of the cat. *MVR.* 19:297–319.

Melder, R. J., L. L. Munn, S. Yamada, C. Ohkubo, and R. K. Jain. 1995. Selectin- and integrin-mediated T-lymphocyte rolling and arrest on TNF-α-activated endothelium: augmentation by erythrocytes. *Biophys. J.* 69:2131–2138.

Schmid-Schönbein, G. W., Y.-C. Fung, and B. W. Zweifach. 1975. Vascular endothelium-leukocyte interaction. *Circ. Res.* 36:173–184.

Shah, R. K., and A. L. London. 1978. Laminar Flow Forced Convection in Ducts. A Source Book for Compact Heat Exchanger Analytical Data. Academic Press, New York.

Shen, Z., and H. H. Lipowsky. 1997. Image enhancement of the in vivo leukocyte-endothelium contact zone using optical sectioning microscopy. *Ann. Biomed. Eng.* 25:521–535.

Springer, T. A. 1994. Traffic signals for lymphocyte recirculation and leukocyte emigration: the multistep paradigm. *Cell.* 76:301–314.

Sutton, D. W., and G. W. Schmid-Schönbein. 1992. Elevation of organ resistance due to leukocyte perfusion. *Am. J. Physiol.* 262(*Heart Circ. Physiol.* 31):H1646–H1650.

Thompson, T. N., P. L. La Celle, and G. R. Cokelet. 1989. Perturbation of red blood cell flow in small tubes by white blood cells. *Pflügers Arch.* 413:372–377.

Warnke, K. C., and T. C. Skalak. 1990. The effects of leukocytes on blood flow in a model skeletal muscle capillary network. *MVR.* 40:118–136.